Available online at www.sciencedirect.com
SCIENCE DIRECT®
Biomaterials 24 (2003) 2695–2705
Biomaterials
www.elsevier.com/locate/biomaterials

Effect of spark plasma sintering on the microstructure and in vitro behavior of plasma sprayed HA coatings

L.-G. Yu[a], K.A. Khor[a,*], H. Li[a], P. Cheang[b]

[a] School of Mechanical & Production Engineering, Advanced Materials Research Centre (AMRC), Nanyang Technological University, 50 Nanyang Avenue, Singapore 639 798, Singapore

[b] School of Materials Engineering, Advanced Materials Research Centre (AMRC), Nanyang Technological University, Singapore 639 798, Singapore

Received 23 September 2002; accepted 30 January 2003

Abstract

The crystalline phases and degree of crystallinity in plasma sprayed calcium phosphate coatings on Ti substrates are crucial factors that influence the biological interactions of the materials in vivo. In this study, plasma sprayed hydroxyapatite (HA) coatings underwent post-spray treatment by the spark plasma sintering (SPS) technique at 500°C, 600°C, and 700°C for duration of 5 and 30 min. The activity of the HA coatings before and after SPS are evaluated in vitro in a simulated body fluid. The surface microstructure, crystallinity, and phase composition of each coating is characterized by scanning electron microscopy and X-ray diffractometry before, and after in vitro incubation. Results show that the plasma sprayed coatings treated for 5 min in SPS demonstrated increased proportion of β-TCP phase with a preferred-orientation in the (2 1 4) plane, and the content of β-TCP phase corresponded to SPS temperature, up to 700°C. SPS treatment at 700°C for 30 min enhanced the HA content in the plasma spray coating as well. The HA coatings treated in SPS for 5 min revealed rapid surface morphological changes during in vitro incubation (up to 12 days), indicating that the surface activity is enhanced by the SPS treatment. The thickest apatite layer was found in the coating treated by SPS at 700°C for 5 min.

Keywords: Hydroxyapatite (HA); β-Tricalcium phosphate; Plasma sprayed coating; Spark plasma sintering (SPS); In vitro; Simulated body fluid (SBF)

1. Introduction

Hydroxyapatite (HA, $Ca_{10}(PO_4)_6(OH)_2$) is the main constituent of hard tissues such as bones, dentine and enamel [1]. As an implant material HA has been tried, and tested clinically as a bioceramic with unique bioactive and osteoconductive properties. It has similar chemical composition and crystal structure to apatite in the human skeletal system, which enables and facilitates the process of bone substitution and reconstruction [2]. Its identical calcium to phosphorous ratio to natural bone encourages advanced bonding between bony tissues and the implant surface. The presence of a rich calcium and phosphorous environment promotes rapid bone formation within the vicinity of the implant [3]. As a result, HA has a wide range of applications, such as microbial seals in middle ear implants, orbital implants for artificial eyes, percutaneous devices for drug delivery, augmentation in maxillofacial surgery [4], coatings on cylindrical posts for dental implants, artificial ears and coated stems for hip prosthesis [5]. The wide range in applications in the body clearly demonstrates its potency as a viable biomaterial for tissue replacement.

Despite its excellent biocompatibility and efficacious biological fixation to bony tissues, the poor mechanical properties of HA with regards to its brittleness and low fracture toughness restrict its use in load bearing applications [6,7]. Therefore, incorporating HA as a coating on mechanically resilient metallic materials to enhance osseointegration has become the most viable method to actualize the benefits of this material.

Coating a metal prosthesis with HA offers the potential of combining the superior mechanical performance

*Corresponding author. Tel.: +65-6-790-5526; fax: +65-6-791-1859.

E-mail address: mkakhor@ntu.edu.sg (K.A. Khor).

0142-9612/03/$ - see front matter
doi:10.1016/S0142-9612(03)00082-6

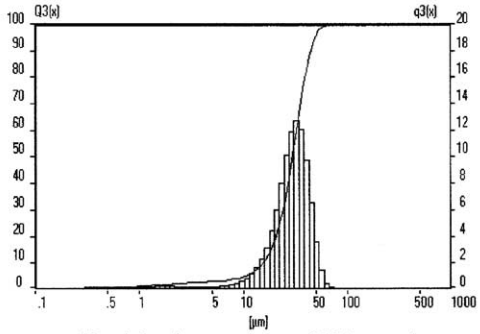

(a) Particle size analysis of HA powder.

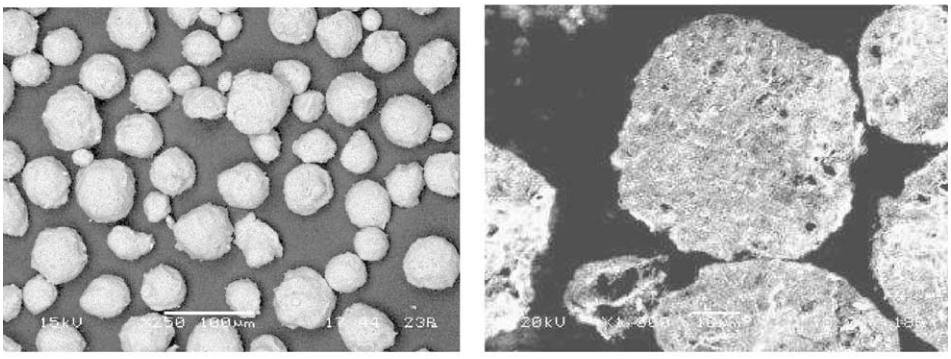

(b) Surface morphology (c) cross-sectional morphology

Fig. 1. Particle size and morphology of starting HA powders: (a) Particle size analysis of HA powder; (b) surface morphology; and (c) cross-sectional morphology.

Table 1
Plasma spray parameters used for preparing HA coatings

Plasma gas	Argon: 1.85 m^3/h
Auxiliary gas	Helium: 1.64 m^3/h
Carrier gas	Argon: 0.3 m^3/h
Net energy	12 kW
Gun current	600–1000 A
Gun transverse speed:	0.25 m/s
Stand off distance	0.08–0.14 m
Powder feed rate	3–3.5 rpm

Table 2
Samples of plasma sprayed HA coatings treated by SPS technique

Sample	SPS temperature (°C)	Duration (min)	Heating rate (K/min)	Punch pressure (MPa)
H-1	500	5	100	10
H-2	600	5	100	10
H-3	700	5	100	10
H-4	700	30	100	10
H-5[a]	—	—	—	—

[a] H-5 is heat treated in an electrical resistance furnace at 700°C for 60 min.

of the metal component with the excellent biological responses possible with the ceramic [8]. HA coatings on metallic substrates such as titanium alloys are widely used for dental and orthopedic implants. There are several advantages of plasma sprayed HA-coated titanium implants. It promotes excellent adhesion between the implant and the contiguous bone, and enhances tissue ingrowth into the pores of HA-coated metallic implant. It eases the formation of strong biological bonds with bony tissues with no concomitant fibrous connective tissue formation. It has excellent biointegration. It facilitates the early load transfer from the implant to the bone. It has a low tendency to evoke cytotoxic responses, and it can protect surrounding bone against metal-ion release from metallic implants [3,9–13].

Plasma spray is widely used to deposit HA coatings, and clinical trials have been conducted to evaluate the capability of these coatings [14]. Yet, owing to the extreme temperatures in the plasma flame (>5000°C), and the rapid cooling of the particles upon impingement on the substrate, the resultant properties of the HA coatings are inadvertently inferior to those of bulk HA [15,16]. The coatings have non-uniform density, and inconsistent adhesion strength. Most importantly, there is uncontrolled decomposition of HA during plasma spray, resulting in significant loss of crystalline HA in the coating. It is well known that the plasma-sprayed HA coating is a mixture of phases such as crystalline stoichiometric HA, amorphous calcium phosphate (ACP), oxyhydroxyapatite (OHA), calcium oxide CaO, α- and β-tricalcium phosphate (TCP) and tetracalcium

phosphate (TTCP) [15,17]. The degree of crystallinity must be controlled, because the crystallinity controls the dissolution/precipitation behavior of the coating.

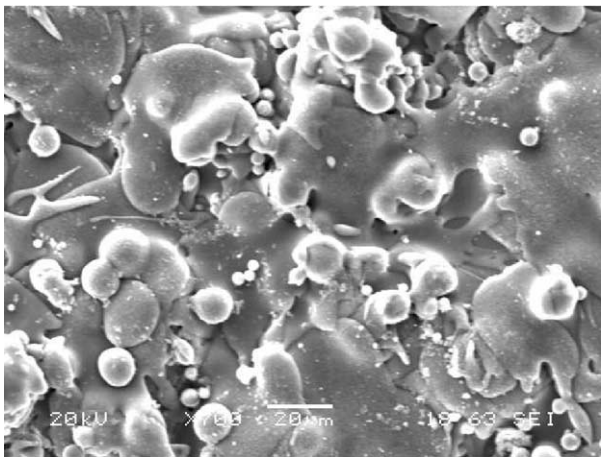

Fig. 2. SEM of As-sprayed HA coating.

Ideally, a bioactive material should have a controlled reactivity that leads to the establishment of a chemical bond with the surrounding tissues [18]. The solubility of a coating must not lead to fast resorption nor should a low reactivity increase the time for bonding to occur. But the crystallinity and the phase composition of plasma sprayed HA coatings are difficult to be controlled by solely controlling the plasma spray processing parameter [19]. Apt post-spray heat treatment is required.

Spark plasma sintering (SPS) is a rapid sintering method, using self-heating phenomena within the powder. It is capable of sintering ceramic powders rapidly to its full density at a relatively lower temperature compared to the conventional furnace sintering method [20–24]. The direct heating of the graphite mold, and the large spark pulse current provide a very high thermal efficiency.

A common characteristic of bioactive ceramic materials is the formation of an apatite layer on their surface

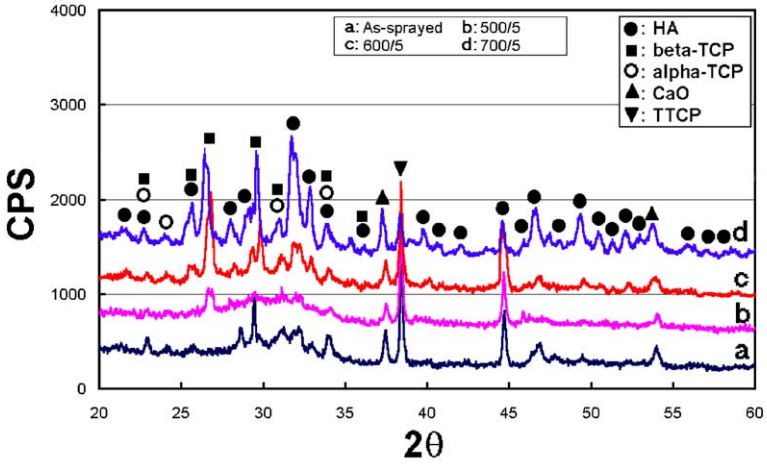

(a) As-received and SPS at 500°C, 600°C, 700°C for 5 minutes,

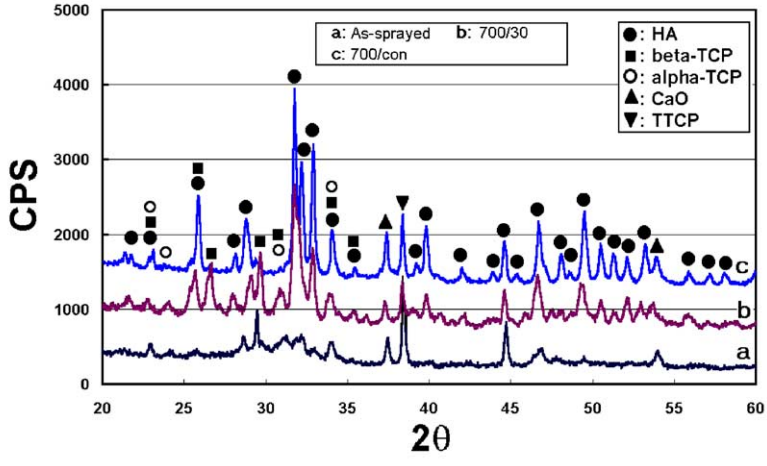

(b) SPS and conventional heat treatment at 700°C for 30 minutes.

Fig. 3. XRD of HA coating samples SPS post-treated at different temperature, holding time and SPS cycle: (a) as-received and SPS at 500°C, 600°C and 700°C for 5 min; and (b) SPS and conventional heat treatment at 700°C for 30 min.

Table 3
Phase composition of selected HA coatings under different post heat treatment[a]

Phases	Samples			
	H-1	H-3	H-4	H-5
	Phase composition of various phase detected in the XRD			
HA	0.5684	0.3629	0.6857	0.8934
Whitlokite (β-TCP)	0.4004	0.6370	0.2211	0.0448
α-TCP	—	—	0.0544	—
CaO	0.0147	—	0.0387	0.0618

[a] The result have not taken the amorphous phase and the preferred orientation into consideration.

when immersed in simulated human blood fluid (SBF) for a period of time [15,17,18,25–28]. The formation of this apatite layer on the surface of the material is an essential requirement for bone bonding, and is related to the solubility of the biomaterials. Both TCP and HA are believed to induce formation of an apatite layer, but the former requires a shorter time to form the film.

In this article, SPS is applied as a post-spray treatment for plasma sprayed HA coating, and the subsequent changes in crystallinity and microstructure are investigated. The in vitro behavior of plasma sprayed HA coating before and after SPS is evaluated. The effect of preferred orientation and crystallinity on the in vitro behavior of the SPS treated coating is

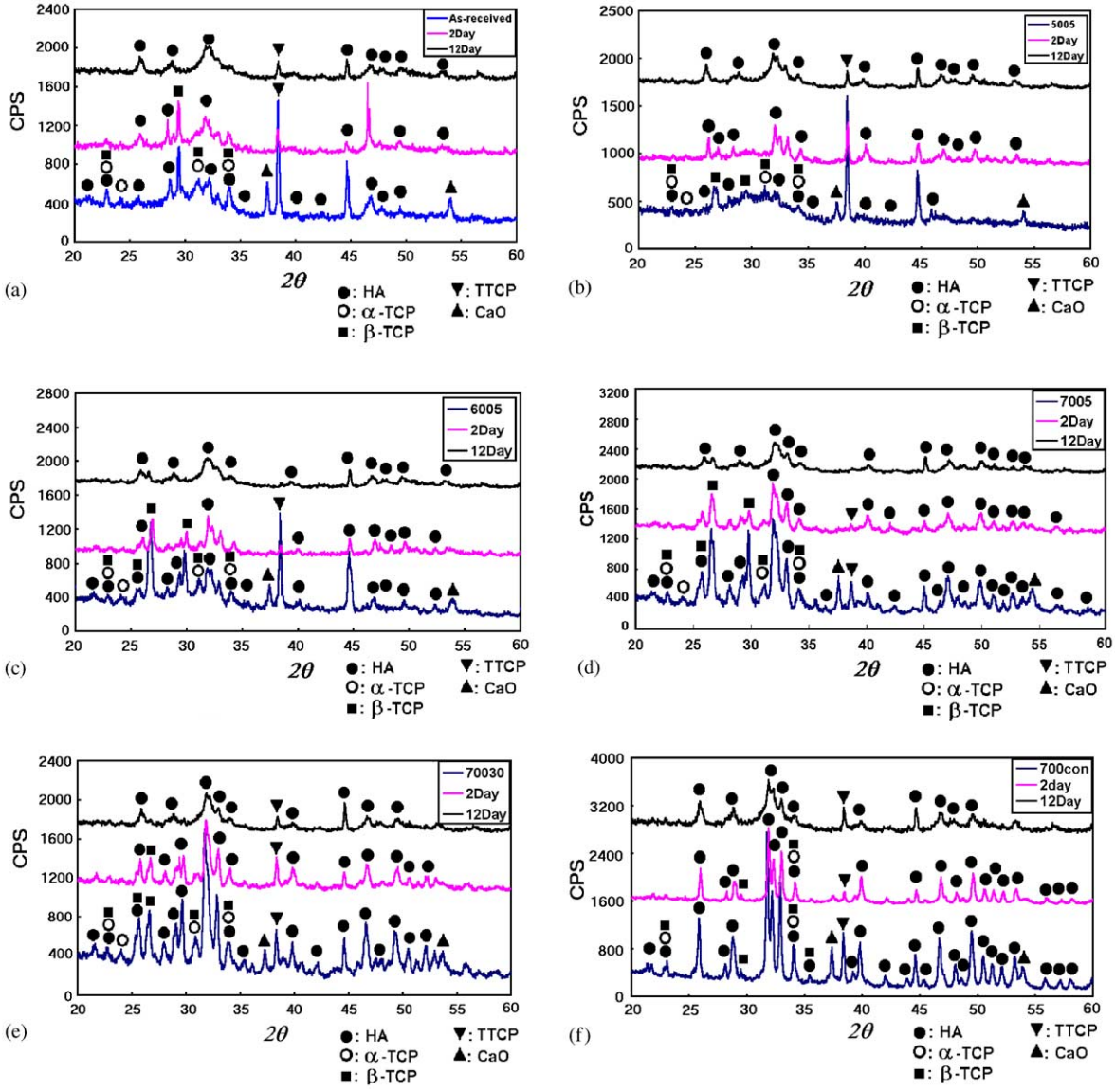

Fig. 4. XRD of HA coating samples SPS post-treated at different temperature, holding time and SPS cycle after in vitro: (a) as-received HA coating; (b) SPS at 500°C for 5 min; (c) SPS at 600°C for 5 min; (d) SPS at 700°C for 5 min; (e) SPS at 700°C for 30 min; and (f) conventional heat treated HA coating.

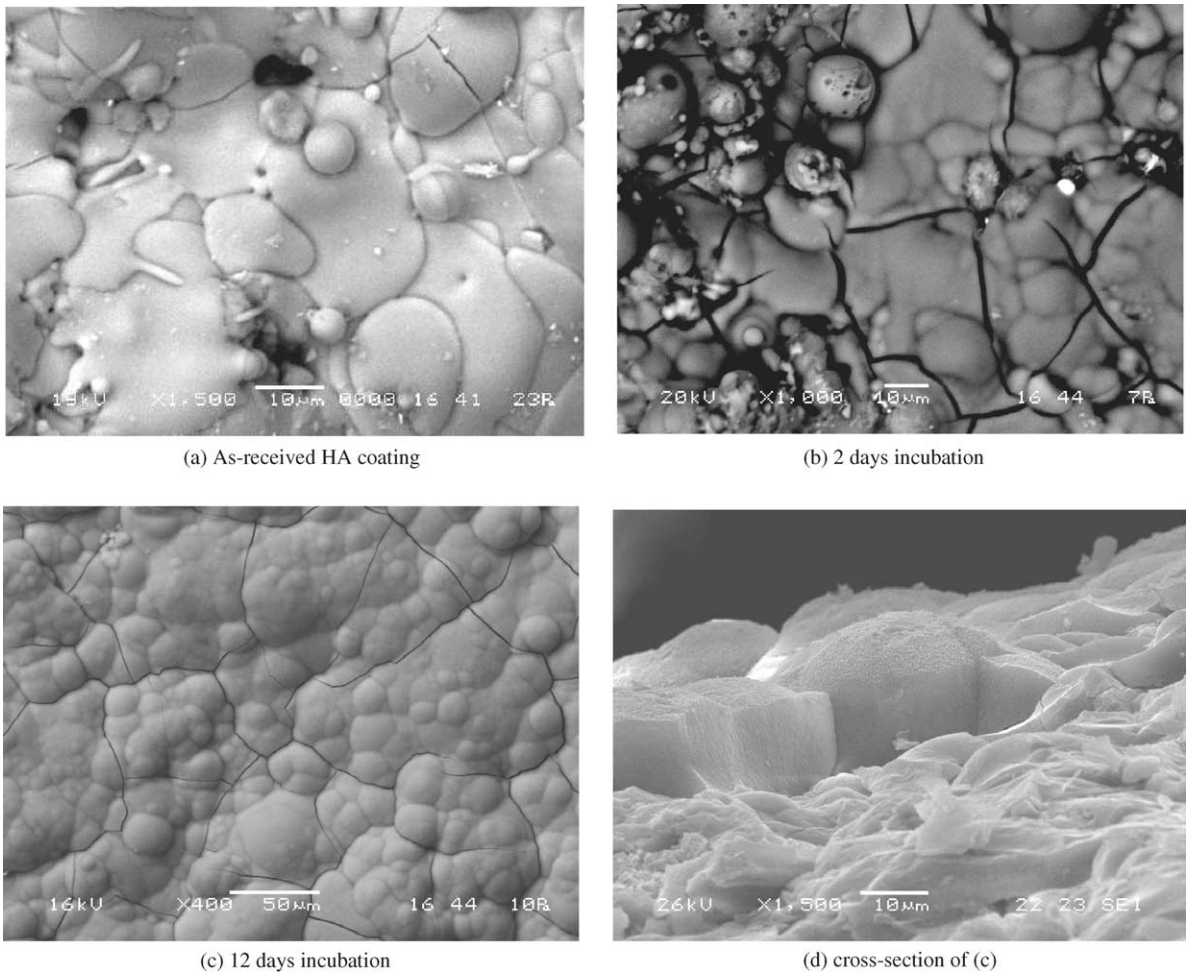

(a) As-received HA coating

(b) 2 days incubation

(c) 12 days incubation

(d) cross-section of (c)

Fig. 5. SEM micrograph of as-sprayed HA coating before and after in vitro: (a) as-received HA coating; (b) 2 days incubation; (c) 12 days incubation; and (d) cross-section of (c).

studied. Also discussed is the possible underlying mechanism responsible for the empirical in vitro behaviors.

2. Experimental materials and procedures

The starting HA powders were made through a wet chemical method and subsequently spray dried to obtain near-spherical powder [29]. The production of the powders is based on the following chemical reaction:

$$6H_3PO_4 + 10Ca(OH)_2 \rightarrow Ca_{10}(PO_4)_6(OH)_2 + 18H_2O. \quad (1)$$

Heat-treatment at 900°C for 1 h is performed to achieve complete crystalline structure. Fig. 1 gives the result of particle size analysis and the morphology of the starting HA powder. The porosity of the HA particle is evaluated by the digital image analysis software Image-Pro Plus (Version 3.0, Media Cybernetics L.P., USA) with the SEM picture of cross-section of the particles, and it is found to be 19.7%.

Ti rod with a diameter of 10 mm is used as the substrate for plasma sprayed HA coatings. The end of Ti rod is cut with a diamond saw and sand blasted before plasma spray to increase the surface roughness in order to get better bonding. The plasma spray parameters are shown in Table 1. The plasma sprayed samples are subsequently cut into 3-mm thick discs, and treated by SPS at various temperatures and duration with a heating rate of 100°C per minute. Table 2 gives the details of SPS parameters for each sample. In the SPS process, the graphite die set is filled with the sample, and placed between the lower and upper electrodes. An external power source provides pulsed current to activate and heat the surface of the particles in the sample for sintering and densification. Charging and discharging the intervals between particles in the sample with electrical energy effectively generate intermittent high temperature spark plasma. The surface microstructure before and after SPS treatment is inspected with SEM. The phase evolution in the HA coating after SPS treatment is checked by XRD. In order to quantify the phase compositions in the HA coatings, the Rietveld

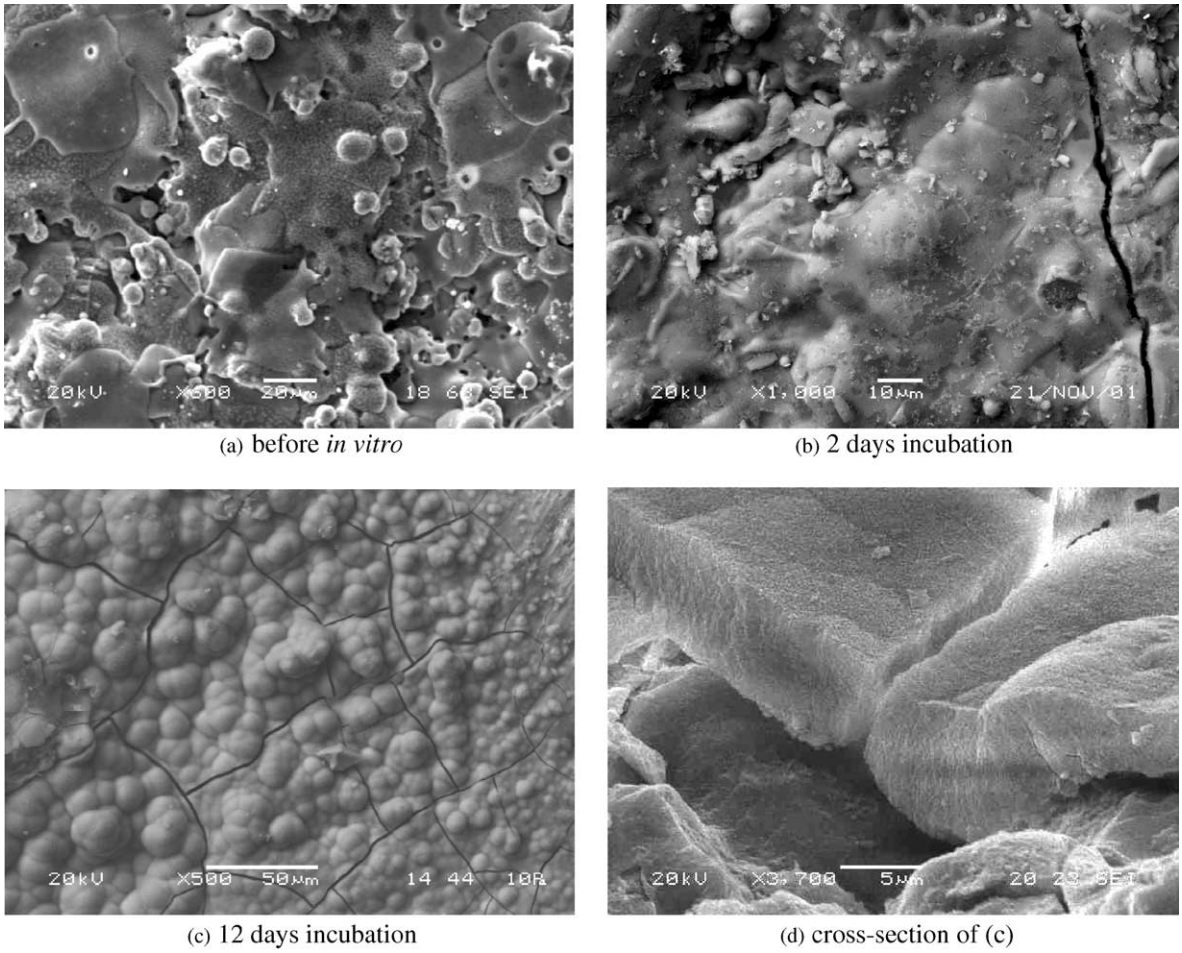

(a) before *in vitro* (b) 2 days incubation

(c) 12 days incubation (d) cross-section of (c)

Fig. 6. SEM micrograph of 500°C/5 min SPS HA coating before and after in vitro: (a) before in vitro; (b) 2 days incubation; (c) 12 days incubation; and (d) cross-section of (c).

method is used to calculate the phase compositions of some of the SPS post-spray treated coatings.

The in vitro tests were conducted to evaluate the bioactivity of the plasma sprayed HA coating post-treated by SPS. An SBF solution that had ionic concentrations close to human blood plasma was prepared by dissolution reagent-grade NaCl, $NaHCO_3$, KCl, K_2HPO_4 ($3H_2O$), $MgCl_2$ ($6H_2O$), $CaCl_2$, and Na_2SO_4, NH_2C $(CH_2OH)_3$ in ion-exchanged distilled water [30]. The solution was buffered at pH 7.4 with 1 N HCl solution at 37°C. The in vitro test was conducted by incubating the samples into a polyethylene bottle containing 70 ml of SBF solution. The bottles were immersed in a continuously stirred distilled water bath container and maintained at a stable temperature of 37°C for periods of 2 and 12 days. The samples were gently rinsed with 1 N HCl and ion-exchanged distilled water, and then dried at room temperature after in vitro testing.

SEM investigated the surface morphology and cross-sectional morphology of the samples after in vitro testing to disclose the histological changes of the coatings. The phase evolution is inspected by XRD.

3. Results and discussion

Fig. 2 displays the surface morphology of as-sprayed HA coating, which is composed of fully melted splats and resolidified micro-droplets.

The XRD inspection for as-sprayed, and SPS post-spray treated HA coatings is shown in Fig. 3. In the as-sprayed coating, the original HA phase apparently decomposed during plasma spray, and phases such as β-TCP, α-TCP, TTCP and CaO are present within the coating. Also, there are large amount of ACP within the coating, as shown in Fig. 3.

XRD results of samples H-1–H-4 show that with increasing SPS temperatures, the crystallinity increased in general, but the phase compositions varies with different SPS temperatures. In H-1, the augmentation of HA phase is not clearly evident, but large amount of β-tricalcium phosphate (β-TCP) with an obvious prefered orientation of the (2 1 4) plane was formed. In H-3, both β-TCP and HA are found to be the dominant calcium phosphate phases, while decidedly more HA phase was found in H-4. The content of α-TCP is very low in all of

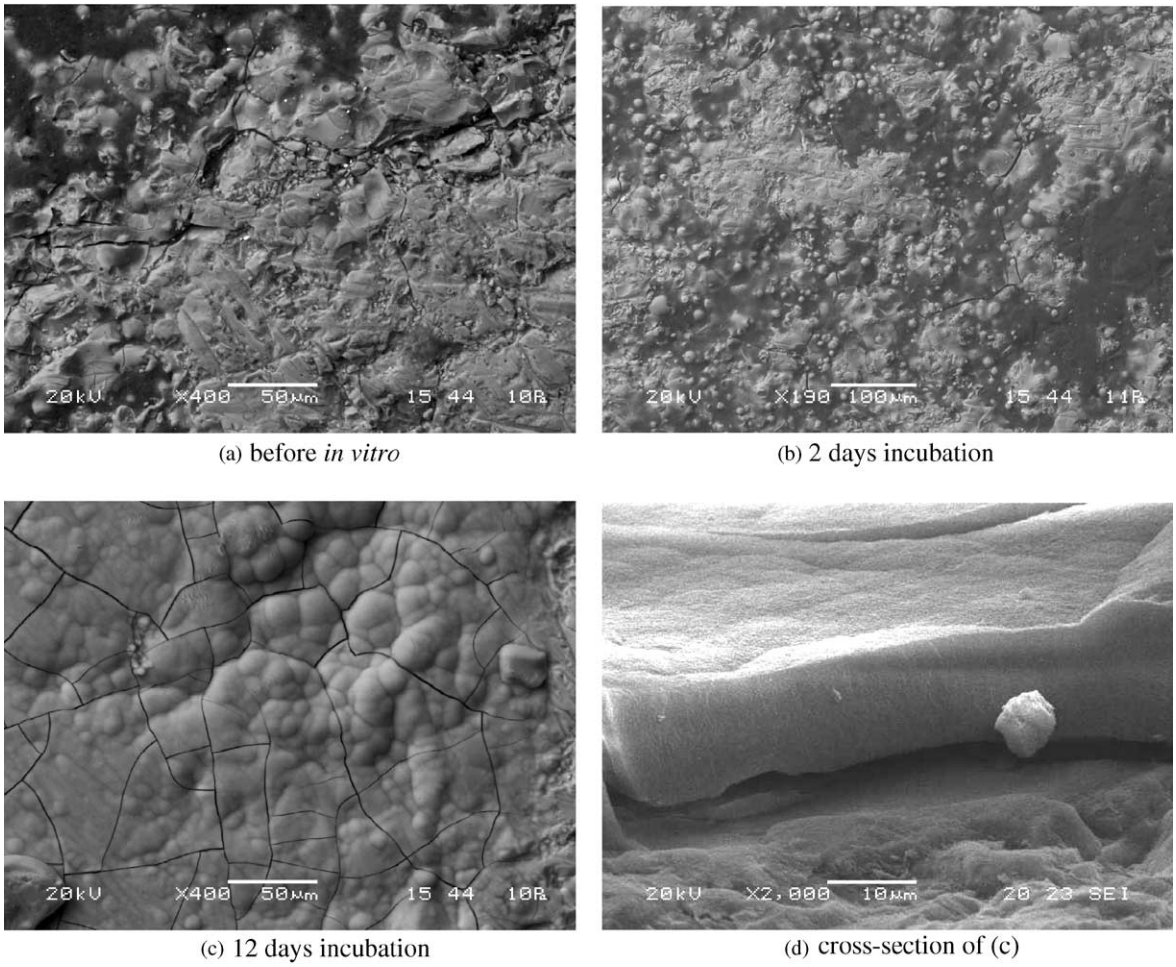

(a) before *in vitro* (b) 2 days incubation

(c) 12 days incubation (d) cross-section of (c)

Fig. 7. SEM micrograph of 600°C/5 min SPS HA coating before and after in vitro: (a) before in vitro; (b) 2 days incubation; (c) 12 days incubation; and (d) cross-section of (c).

the HA coatings. In order to compare the phase composition of the HA coatings, the Rietveld method was applied to quantitatively calculate the contents of phase within selected HA coatings. The results are shown in Table 3. Fazan et al. [15] reported that firing the plasma sprayed coating at 600°C for 1 h in conventional electric resistant furnace increases the crystallinity of the coatings to almost 100%. The authors also find that, for HA coating post-spray treated by conventional heat treatment, the HA phase composes nearly 90 wt% of the crystalized phase (Table 3) in the coating. But SPS has a different effect on plasma sprayed coating. For example, H-2 and H-3 do not show fully crystalline HA as the main phase in the coating, but show the formation of preferred-oriented β-TCP. Particularly, in H-3 the crystallized phases mainly composed of β-TCP, which is about 64 wt% (Table 3). This phenomena may be contributed by the unique heating feature of the SPS process. In conventional vacuum furnance heat treatment, the heating process is a near-equilibrium heating process, which ensures the annealing-recrystalization of meta-stable apatite phases in plasma sprayed coating, and the stable HA phase is obtained ultimately. In the SPS process, the large electrical current and the apparent plasma induced by the discharge at the micro-gap between graphite punch and coating surafce produces a nonequlibrium electrothermal effect, which stimulates the evaporation/condensation of surface material. The evaporation-condensation of the surface apatite layer ensures the metastable phases like β-TCP to growth with its preferred orientation. Because the growth of apatite layer by evaporation/condensation is an epitaxial growth rather than a recrystalization or rapid solidification process, both the stable HA phase and the unstable amorphous are reduced in the coating. The plasma effect is only eminent at the beginning of SPS process. This is because the discharge in the SPS process is only taking place at the very onset of the SPS process, and when a stable electric path is established in the electrode–punch–coating–substrate–punch–electrode route, there is no discharge on the coating surface any more. The electrothermal effect works just like the heat effect in conventional vacuum furnace, and the

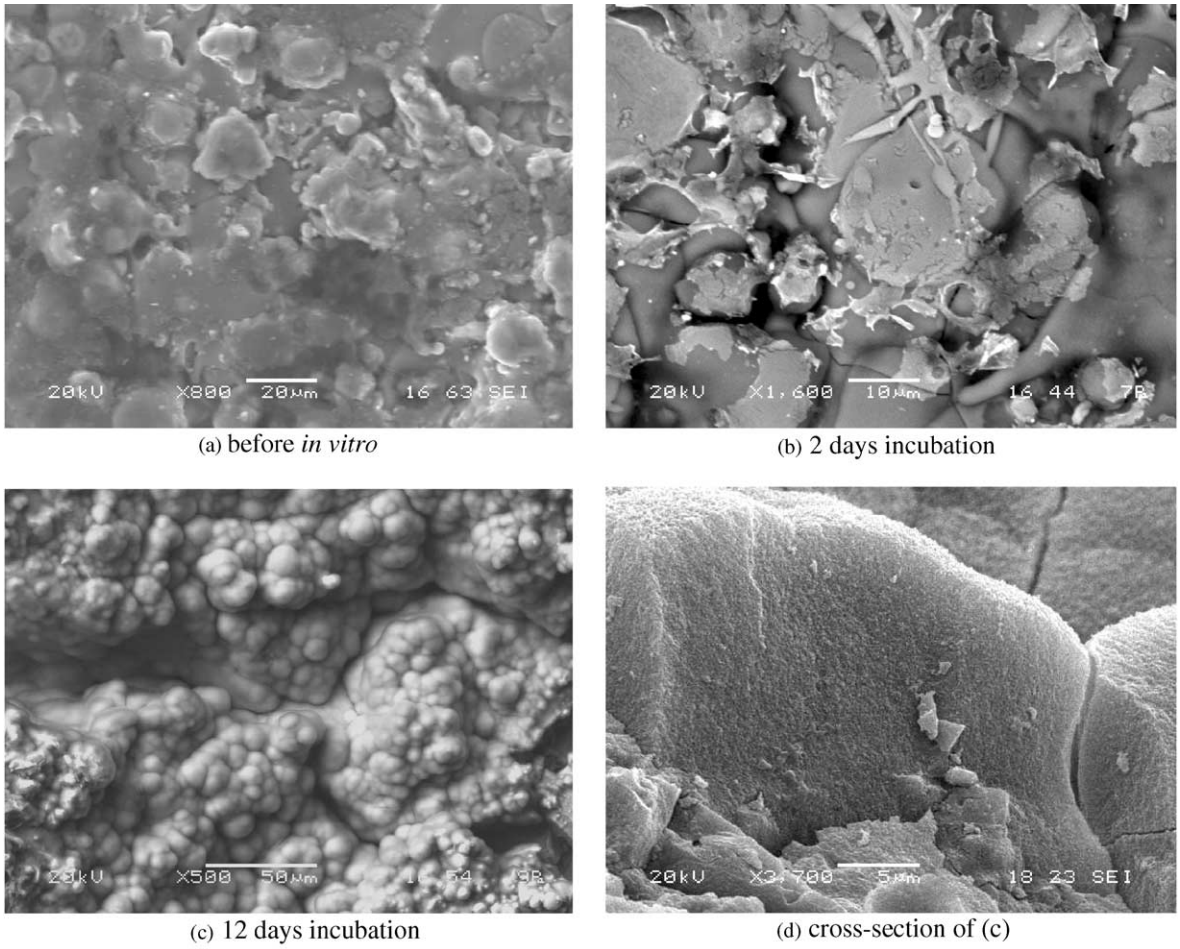

(a) before *in vitro* (b) 2 days incubation

(c) 12 days incubation (d) cross-section of (c)

Fig. 8. SEM micrograph of 700°C/5 min SPS HA coating before and after in vitro: (a) before in vitro; (b) 2 days incubation; (c) 12 days incubation; and (d) cross-section of (c).

annealing/recrystallization will dominate the phase transformation process. This is the reason why, for sample H-4, the HA content increase significantly to approximately 70 wt% (Table 3).

The phase evolution on the surface of HA coatings induced by in vitro aging were studied by XRD, and were shown in Fig. 4. For the as sprayed and all SPS treated HA coatings, the dissolution of TCP, TTCP and CaO evidently took place during the first two days of incubation, which is indicated through the eminent decrease of peak intensity of these phases. After 12 days, all the samples have an apatite layer grown on the surface. Yet, for the as-sprayed coating and H-1, the peak referring to TTCP was still evident after 12 days of incubation. Similar result is also revealed by H-4. XRD result shows that in H-4, although there is also dissolution of TCP, TTCP and CaO, the precipitation rate of the new layer is sedately gradual, and the peaks assigned to the HA phase remained sharp and narrow after 12 days of incubation.

Figs. 5–9 show the surface morphology of SPS treated HA coatings before, and after in vitro incubation. The cross-sectional morphology of the HA coating samples after 12 days of incubation is also presented. The morphology for the HA coating after conventional heat treatment at 700°C for 1 h is shown as Fig. 10 together with the in vitro incubation result.

For HA coating SPS treated at a temperature as low as 500°C, the droplet surface became irregular, indicating phase transformation took place on the surface, as shown in Fig. 6. At SPS temperature of 700°C, the droplet surface becomes even more uneven, and microcracking is found in the coating, indicating further phase transformations took place after SPS post-treatment at higher temperature.

In vitro results indicate that, for all HA coatings including as-sprayed SPS treated and conventional heat-treated coatings, there is an apatite layer grown on the surface of HA coating. Yet the apatite layer thickness for different HA coatings are diverse. Table 4 provides the apatite layer thickness grown on the HA coatings after 12 days of incubation. It can be seen that, the growth of apatite layer on H-3 is the thickest, with a layer thickness of about 16 μm. And the growth of

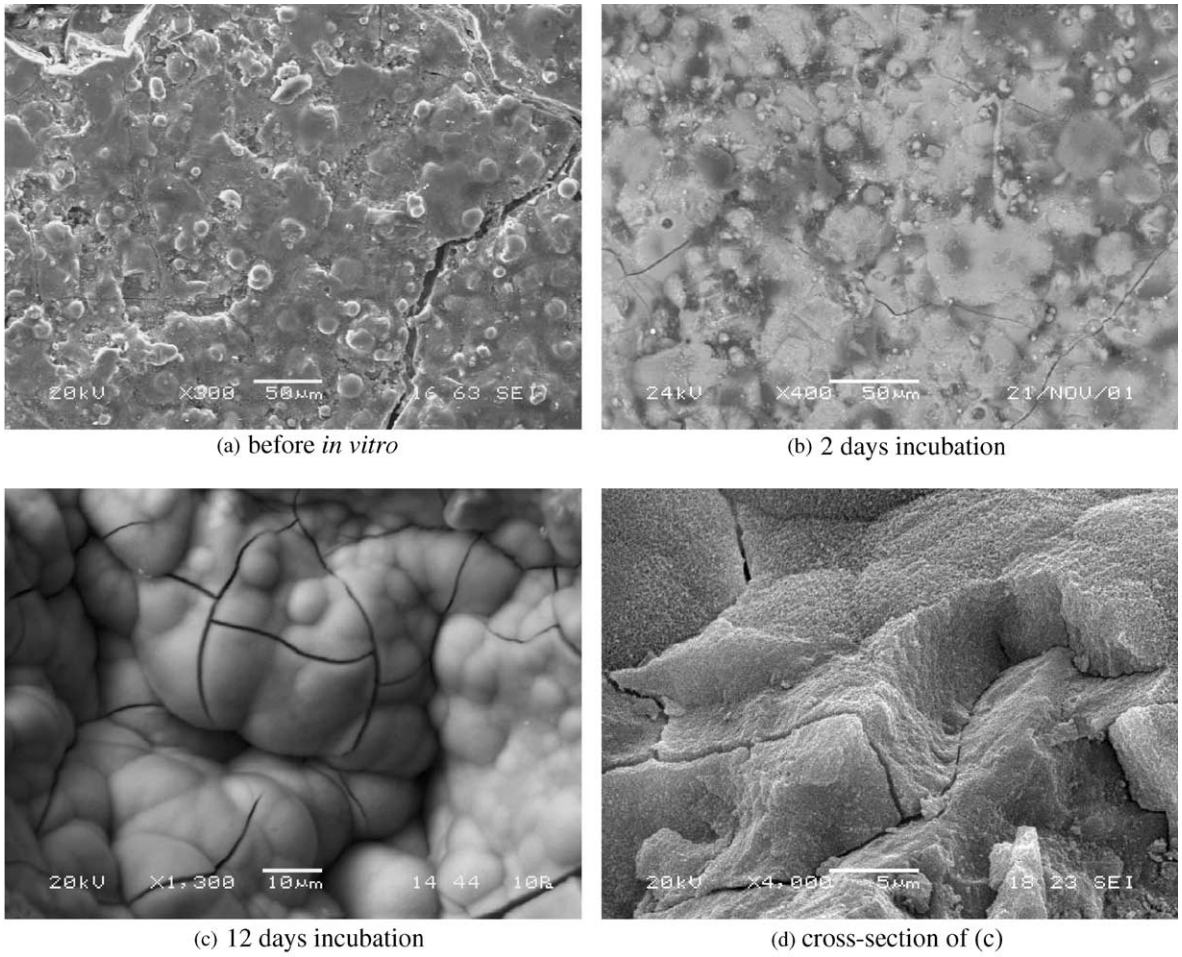

Fig. 9. SEM micrograph of 700°C/30 min SPS HA coating before and after in vitro: (a) before in vitro; (b) 2 days incubation; (c) 12 days incubation; and (d) cross-section of (c).

apatite layer on H-5 is the thinnest, with a new apatite layer of about 3.5 μm. It is believed that this behavior was related to the higher solubility of TCP, CaO and TTCP, and the lower solubility of the stable HA phase. As samples H-1–H-3 retained more metastable phases such as β-TCP as compared to H-5, the dissolution process is likely to proceed faster in SPS treated coatings, and subsequently, the SBF solution attained supersaturation of Ca^{2+} and HPO_4^- ions rapidly. This caused the precipitation of apatite layer to progress more rapidly on H-1–H-4 than on H-5.

The observed surface structural changes of HA coatings upon SPS and conventional heat treatment, and the related in vitro behavior could be explained by virtue of the Kelvin–Gibbs free energy relationship. The initial nucleation process, which determines the size, number, and morphology of the precipitating crystals, has to create new surfaces. This process requires the energy provided by the free energy term due to the tendency of the supersaturated solution to deplete itself by deposition. Therefore, there is an energy balance between the formation of the solid phase and the deposition process. At the point where these free energies are equal, critical clusters, which have an equal opportunity to grow or dissolve, are formed. Clusters larger than the critical size will tend to grow since the surface energy term becomes less important as the size increases. Once the critical size has been reached by aggregation, the super-saturation is rapidly depleted and these crystallites will tend to grow by a process of crystal growth. Thus, it is extremely sensitive to super-saturation. Below the critical super-saturation the nucleation will not happen, but once this value is attained, the rate increases very rapidly. It is therefore easy to see that the critical super-saturation is the controlling factor in this process. Also the critical super-saturation varies according to different calcium phosphate crystal structures. This is because different crystal structures have different surface energy, and nucleation on a higher energy surface will generally require a smaller driving force. In other words, a lower supersaturation is needed for the induction of nucleation on a low energy surface than that for the induction of nucleation on a high energy, such as a well-crystallized surface. According to XRD

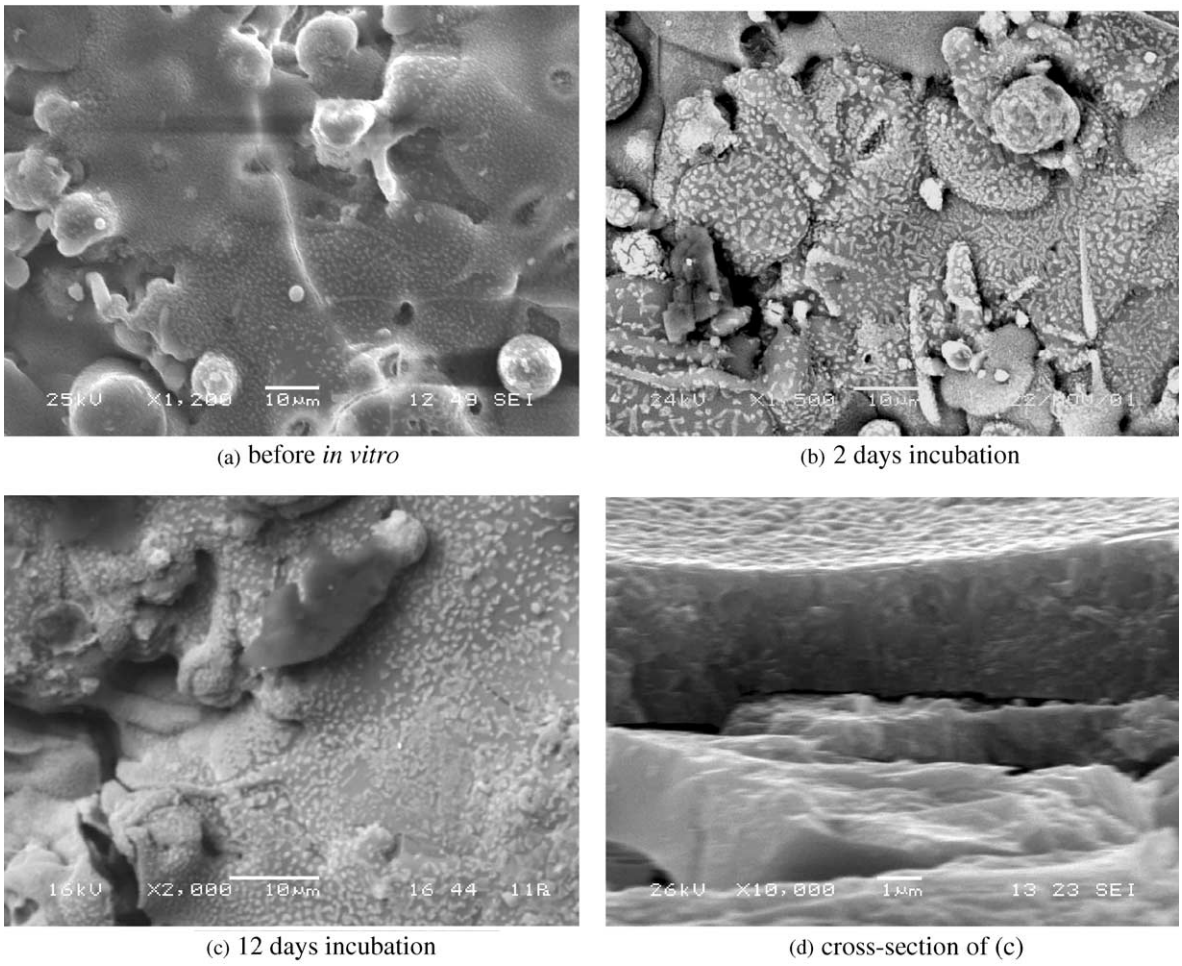

Fig. 10. SEM micrograph of SPS HA coating post-spray treated by conventional heat treatment: (a) before in vitro; (b) 2 days incubation; (c) 12 days incubation; and (d) cross-section of (c).

Table 4
Apatite layer thickness on different HA coatings after 12 days incubation in SBF

Sample	Apatite layer thickness (μm)
As-Sprayed	12.0
H-1	7.1
H-2	12.7
H-3	16.1
H-4	5.3
H-5	3.5

analysis, the as-sprayed coating, and coatings SPS treated at 500°C, 600°C and 700°C for 5 min (H-1, H-2, and H-3) are mostly composed of amorphous or metastable phases with many crystal defects. On the other hand, HA coatings after SPS at 700°C for 30 min, and after conventional heat treatment (H-4 and H-5) contain more HA phase. The higher dissolution rate and lower supersaturation requirement ensures faster precipitation of the apatite layer on H-1, H-2 and H-3 than H-4 and H-5. The aforementioned result shows that SPS treatment can activate the surface of the plasma sprayed coating, and make the dissolvation/precipitation of new apatite layer on plasma sprayed coating during immersion in SBF proceed faster, and ultimately, a thicker apatite layer.

4. Conclusions

Spark plasma sintering (SPS) post-spray treatment of plasma sprayed HA coatings yields the following findings:

1. The crystallinity of calcium phosphate phases increased overall after SPS treatment. Yet, brief SPS treatment duration (H-1 and H-3) aided the formation of metastable β-TCP phase with obvious preferred orientation in the (214) plane, and the content of β-TCP phase increased with correspondingly with SPS temperature. On the other hand, relatively prolonged SPS duration (H-4) assists the formation of HA phase in the plasma sprayed coatings. Conventional heat treatment at 700°C

for 1 hour (sample H-5) also helps the formation of HA phase.

2. In vitro incubation results show that the precipitation of apatite layer on samples H-1, H-2 and H-3 is more rapid than that on plasma sprayed HA coatings with extensive SPS treatment (H-4) and coating with conventional heat treatment (H-5). The HA coating treated in SPS at 700°C for 5 min (H-3) featured the thickest apatite layer (16.1 μm).
3. The SPS parameters employed in the present study demonstrated that plasma sprayed HA coating could be activated for interaction with the SBF, which in return result in accelerated growth of apatite layer on the surface.

Acknowledgements

Financial assistance from Nanyang Technological University in the form of research project no. RG 78/98 is gratefully recognized.

References

[1] Ravaglioli, Krajewski A. Bioceramics: materials, properties, applications. Chapman & Hall, London, 1992.
[2] Aoki. Medical applications of hydroxyapatite. Ishiyaku Euro-America, Inc., Japan, 1994. p. 290–291.
[3] Gross KA, Berndt CC. Thermal processing of hydroxyapatite for coating production. J Biomed Mater Res 1998;39:580–7.
[4] Khor K, Cheang P, Wang Y. The thermal spray processing of HA powders and coatings. J Min Met Mater Soc 1997;49:51–7.
[5] Cronin RJ, Oesterle LJ, Ranly DM. Mandibular implants and the growing patient. Int J Oral Maxillofac Implants 1994;9:55–62.
[6] Weng J, Liu XG, Zhang XD, De Groot K. Integrity and thermal deposition of apatites in coatings influenced by underlying titanium during plasma spraying & post-heat-treatment. J Biomed Mater Res 1996;30:5–11.
[7] Chang, Shi J, Huang J, Hu Z, Ding C. Effects of power level on characteristics of vacuum plasma sprayed hydroxyapatite coating. J Therm Spray Tech 1998;7(4):484–8.
[8] Ji H, Taylor M, Chandler P, Ponton CB, Marquis PM. The microstructure of plasma sprayed hydroxyapatite. In: Doherty PJ, Williams RL, Williams DF, Lee AJC, editors. Biomaterial—tissue interfaces. Advances of biomaterials, vol. 10. Amsterdam: Elsevier Science, 1992. p. 165–9.
[9] Yang CY, Wang BC, Chang E, Wu JD. The influences of plasma spraying parameters on the characteristics of hydroxyapatite coatings: a quantitative study. J Mater Sci: Mater Med 1995;6:249–57.
[10] Park E, Condrate RA, Hoelzer DT. Interfacial characterization of plasma sprayed coated calcium phosphate on Ti–6Al–4V. J Mater Sci: Mater Med 1998;9:643–9.
[11] Khor KA, Wang Y, Cheang P. Thermal spraying of functionally graded coatings for biomedical applications. Surf Eng 1998; 14(2):159–64.
[12] Wang BC, Chang E, Lee TM, Yang CY. Changes in phases and crystallinity of plasma-sprayed hydroxyapatite coatings under heat treatment: a quantitative study. J Biomed Mater Res 1995;29:1483–92.
[13] Sousa SR, Barbosa MA. Effect of hydroxyapatite thickness on metal ion release from Ti–6Al–4V substrates. Biomaterials 1996; 17:397–404.
[14] Lewis G. Hydroxyapatite-coated bioalloy surfaces: current status and future challenges. Bio-Med Mater Eng 2000;10: 157–88.
[15] Fazan F, Marquis PM. Dissolution behavior of plasma-sprayed hydroxyapatite coatings. J Mater Sci: Mater Med 2000; 11:787–92.
[16] Palka V, Postrkova E, Koerten HK. Some characteristics of hydroxylapatite powder particles after plasma spraying. Biomaterials 1998;19:1763–72.
[17] Chou L, Marek B, Wagner WR. Effects of hydroxylapatite coating crystallinity on biosolubility cell attachment efficiency and proliferation in vitro. Biomaterials 1999;20:977–85.
[18] Carvalho FLS, Borges CS, Roberto J, Branco T. J Non-Cryst Solids 1999;247:64–8.
[19] Prevey PS. X-ray diffraction characterization of crystallinity and phase composition in plasma-sprayed hydroxyaptite coatings. J Therm Spray Technol 2000;9(3):369–76.
[20] Johnson, Lynn D. Microwave and plasma sintering of ceramics. Ceram Int 1991;117(5):295–300.
[21] Risbud SH, Shan CH. Fast consolidation of ceramic powders. Mater Sci Eng A 1995;204:146–51.
[22] Hong J, Gao L, Torre SDDL, Miyamoto H, Miyamoto K. Spark plasma sintering and mechanical properties of ZrO_2 (Y_2O_3)–Al_2O_3 composites. Mater Lett 2000;43:27–31.
[23] Shan CH, Risbud SH. Rapid consolidation of Bi–Pb–Ca–Cu–O powders by a plasma activated sintering process. Mater Sci Eng B 1994;26:55–60.
[24] Gao L, Wang HZ, Hong JS, Miyamoto H, Miyamoto K, Nishikawa Y, de la Torre SD. SiC–ZrO_2 (Y)–Al_2O_3 nanocomposites superfast densified by spark plasma sintering. Nanostruct Mater 1999;11(2):43–9.
[25] Santos JD, Reis RL, Monteiro FJ, Knowles JC, Hastings GW. Liquid phase sintering of hydroxyapatite by phosphate and silicate glass additions: structure and properties of the composites. J Mater Sci: Mater Med 1995;6:348–52.
[26] Arciola R, Montanaro L, Moroni A, Giordano M, Pizzoferrato A, Donat M. Hydroxyapatite-coated orthopaedic screws as infection resistant materials: in vitro study. Biomaterials 1999;20:323–7.
[27] Ferraz MP, Fernandes MH, Trigo Cabral A, Monteiro FJ. In vitro growth and differentiation human bone marrow cells on hydroxyapatite plasma-sprayed. J Mater Sci: Mater Med 1999;10:567–76.
[28] Luo ZS, Cui FZ, Feng QL, Lia HD, Zhu XD, Specto M. In vitro and in vivo evaluation of degradability of hydroxyapatite coatings synthesized by ion beam-assisted deposition. Surf Coat Technol 2000;131:192–5.
[29] Kweh SWK, Khor KA, Cheang P. Production and characterization of hydroxyapatite (HA) powders. J Mater Process Technol 1999;89–90:373–7.
[30] Kokubo T, Kushitani H, Sakka S, Kitsugi T, Yamamuro T. Solutions able to reproduce in vivo surface changes in bioactive glass-ceramic A-W3. J Biomed Mater Res 1990; 24:721–4.